Journal of Applied Fluid Mechanics, Vol. 13, No. 1, pp. 15-23, 2020.
Available online at www.jafmonline.net, ISSN 1735-3572, EISSN 1735-3645.
DOI: 10.29252/jafm.13.01.29777

Numerical Study of Particle Dispersion in the Turbulent Recirculation Zone of a Sudden Expansion Pipe using Stokes Numbers and Mean Drift Parameter

M. J. Torres[1†], J. García[2] and Y. Doce[3]

[1] *Escuela de Ingeniería Mecánica. Pontificia Universidad Católica de Valparaíso, Chile*
[2] *Grupo de Investigación de Mecánica de Fluidos aplicada a la Ingeniería Industrial, Universidad Politécnica de Madrid, Madrid, 28006, Spain*
[3] *Departamento de Ingeniería Mecánica, Química y Diseño Industrial. Escuela Técnica Superior de Ingeniería y Diseño Industrial. Universidad Politécnica de Madrid, Madrid, 28012, Spain*

†*Corresponding Author Email: josefina.torres@pucv.cl*

(Received October 22, 2018; accepted April 16, 2019)

ABSTRACT

The dispersion of solid particles in zones of turbulent recirculation flow is of interest in various technological applications. Many experimental studies have been developed in order to know the contribution of Stokes numbers and mean drift parameter on the entering and dispersion of particles in the recirculation zone however to our knowledge there are not numerical studies reported about it. In this work, we made a numerical study of the incompressible turbulent flow laden with solid particles in sudden expansion pipes with different expansion ratios and different Reynolds number upstream of the pipe, using LES and Germano dynamic model with JetCode program for the continuous phase (air). The solid particles movement (different diameters were considered) was solved by using a Lagrangian tracking algorithm coupled to JetCode taking into account only drag and gravity forces supposing one way coupling. Finally, we calculated Stokes numbers based on the different fluid time scales and the mean drift parameter for all the solved cases and studied their isolated effect on the solid particle dispersion in the recirculation zones by computing the concentration by means of the particle number within the recirculation zones. Our results coincided with the experimental findings reported by others authors: the particle concentration exhibits a maximum value as the Reynolds number upstream in the pipe is decreased, the pipe expansion ratio is increased and particle size is decreased. Regarding the results obtained numerically about the solid particle dispersion within turbulent recirculation zones in terms of Stokes numbers and the mean drift parameters, coincided adequately with the experimental results.

Keywords: Turbulent flow; Sudden expansion pipe; Particle concentration; Multiphase flow.

NOMENCLATURE

C_f	friction coefficient at the wall expansion
C_{pr}	particle concentration in the recirculation zone
H	step size
L_e	length of the exit pipe
L_i	length of the inlet pipe
N_{pr}	number of particles in the recirculation zone
R	radius of inlet pipe
R_e	radius of exit pipe (expansion)
Re_b	bulk Reynolds number
Re_p	particle Reynolds number
S_{tr}	transit Stokes number
S_ω	centrifugal Stokes number
St_e	large eddy Stokes number
$\boldsymbol{u}$	fluid velocity vector
U_b	bulk fluid velocity
U_C	average fluid velocity at the center of the expansion
U_e	bulk fluid velocity in the expansion
$\boldsymbol{u}_p$	particle velocity vector
$\mathbf{u}_T$	terminal velocity of particles
$\boldsymbol{x}_p$	particle position vector
x_r	reattachment length
τ_p	particle relaxation time

1. INTRODUCTION

The existence of diverse industrial applications that involve the flow with particles through a pipe with a sudden expansion together with the complexity of the flow and the phenomena that take place in it (It combines a region of strong non-equilibrium, the recirculation zone, followed by a region where the flow returns to equilibrium), make this study very interesting and useful. Many researches are available in the literature on this subject: Tashiro and Tomita (1986), Ahmadi and Chen (1998), Founti and Klipfel (1998), Aguinaga *et al.* (2008), Terekhov and Pakhomov (2008), Mergheni *et al.* (2012), Pakhomov and Terekhov (2013) and El-Askary *et al.* (2015). In this review, the study of flow laden with particles through this geometry, has been mostly experimental whereas numerical studies have been developed in a two-dimensional domain, and most of them as two-equation turbulence models. The study of particle dispersion within turbulent recirculation zones in a sudden expansion pipe is important because the turbulent flow laden with solid particles appears in many technological applications and it can be characterized by different Stokes numbers and mean drift parameters. Many experimental studies have been developed in order to know the contribution of Stokes numbers on the entering and dispersion of particles in the recirculation zones, Hardalupas *et al.* (1992), experimentally studied the dispersion of glass beads in an air flow through sudden expansion pipe in the direction of gravity by investigating with phase-Doppler anemometry, which provided velocity measurements and characteristics of the concentration. Additionally, they studied the effect of the Stokes numbers based on different fluid timescales showing how these parameters controlled the particle dispersion in the recirculation zone. Lau and Nathan (2014) measured the influence of Stokes number on the distributions of particle concentration and velocity at the exit of a long pipe, the data were obtained by using particle image velocimetry and planar nephelometry, simultaneously. With respect to the mean drift parameter Wang and Stock (1993), developed a simple mathematical and physical analysis of the dispersion statistics of heavy particles in a homogeneous and isotropic turbulent flow in terms of measurable flow Eulerian scales, particle inertia and particle drift velocity. Siu *et al.* (2011), measured the trajectories of particles into, and around, the recirculation zone formed in water flowing through a sudden pipe expansion with radius ratio 1:3.7 with Reynolds numbers between 5,960 and 41,700 over a wide range of Stokes numbers. Their findings confirmed that the effect of increasing the drift parameter was to reduce the trend of the particles to enter the recirculation zone. As far as we know there are not numerical studies reported about the influence of Stokes numbers and drift parameter on the solid particle dispersion within the recirculation zone in a sudden expansion pipe. In this paper, we developed a numerical study by using LES and Lagrangian tracking to simulate the incompressible and turbulent flow laden with solid particles with diameters $dp_1 = 60\ \mu m$ and $dp_2 = 150\ \mu m$ in sudden expansion pipes with different step size ($H_1 = 2,\ H_2 = 2.5$) and different Reynolds number upstream the pipe ($Re_{b1} = 10600, Re_{b2} = 14000$). Also, we calculated Stokes numbers based on the fluid time scales corresponding to large eddy (St_e), transit along the recirculation zones (St_{tr}) , centrifugal (St_ω) and mean drift parameter (γ_{mean}) for all the solved cases. Finally, we studied their isolated effect on the particle dispersion in the recirculation zones by computing the different concentrations (by means of the particle number within the recirculation zone, Torres, 2014).

The document is organized as follows. Firstly, in the section 2, we will describe the physical model and numerical methodology. After that, in Section 3, we will show the velocity statistics of fluid and particles of the studied cases. Finally, the characterization of the entering and the increase of particle concentration within the recirculation zone with different formulations of Stokes number and mean drift parameter of solid particles will be provided in Section 4. Last section summarizes the main results and conclusions.

2. PHYSICAL MODELLING AND NUMERICAL METHODOLOGY

In the present work, the JetCode program was used; which was originally formulated to solve only the gas turbulent flow through channels and pipes. Therefore, in order to simulate the solid particle laden flow a couple of subroutines were developed describing the solid particle movement. To validate the new implemented code three different configurations were tested: plane channel, channel with a step and straight pipe. The results obtained numerically were compared against experimental data available in the bibliography (turbulent flow laden with solid particles through: plane channel (Kulick *et al.*, 1994), channel with a step (Fessler and Eaton, 1997), straight pipe (Marchioli *et al.*, 2003) and a good agreement was found. For more details, see Torres (2014). In this paper a sudden expansion was taken into consideration, the flow has similar characteristics of previous flows and it is assumed the code will behave correctly.

The computational domain consists of an inlet pipe of radius R and length L_i with a sudden expansion into an outlet pipe of radio R_e, length L_e and step size is $H = R_e - R$. The origin of the coordinate system is located at the central point of the cross-section at the expansion, $x = 0$; x, θ and r axes represent streamwise, spanwise and wall-normal directions, respectively (see Fig. 1). Samples of pointwise and monodisperse heavy particles with density $\rho = 2500\ kg.m^{-3}$ and diameters $dp_1 = 60\ \mu m$, $dp_2 = 150\ \mu m$ are injected into the flow at the injection area indicated in Fig. 1. The flow laden with particles is vertical and it is aligned with gravity acceleration, $\boldsymbol{g} = g_x \hat{\imath}$.

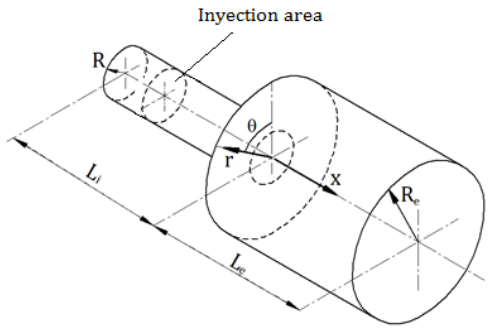

Fig. 1. Geometry scheme.

The length of the downstream pipe (Le) has been taken long enough to ensure that the expansion effects are vanished before pipe exit. Four different geometric configurations have been solved in this study (see Table 1).

Table 1 Dimensions of flow configurations

	$R\ (m)$	L_i/R	ER	L_e/R	H/R
$Re_{b1}H_1$	0.025	4	3	40	2
$Re_{b1}H_2$	0.025	4	3.5	50	2.5
$Re_{b2}H_1$	0.0075	10	3	35	2
$Re_{b2}H_2$	0.0075	10	3.5	40	2.5

Periodic boundary conditions are imposed on the fluid velocity field in the azimuthal homogeneous direction (θ) which implies that the flow is fully developed and statistically steady in space, it can be expressed as $\mathbf{u}(r,\theta,z) = \mathbf{u}(r,\theta + L_\theta, z)$ with $L_\theta < 2\pi$, no slip boundary conditions are imposed at the pipe walls and a convective condition at the exit $\frac{\partial u_i}{\partial t} + U_c \frac{\partial u_i}{\partial n} = 0$, where U_C is the convection velocity and η is the coordinate in the direction of the outward normal at the boundary (Pierce and Moin, 2004). No-slip boundary conditions are imposed at the pipe walls and convective condition at the exit pipe.

We consider non-reactive, isothermal and incompressible flow (low Mach number). The air density is ρ and kinematic viscosity ν, the bulk Reynolds number is $Re_b = U_b 2R/\nu$ based on the bulk velocity U_b and diameter of the inlet pipe $2R$. At the inlet, a fully developed turbulent velocity profile was imposed; it was obtained from a previous simulation of turbulent flow through a straight pipe with the same diameter and Re_b using the program JetCode.

2.1 Equations for Fluid Phase and Flow Solver

Continuity and momentum equations in cylindrical coordinates filtered by LES are discretized in a three-dimension way by using the finite volume method with a structured hexahedral mesh and solved implicitly within JetCode program (Pierce and Moin, 2001). The subgrid scale is solved using the dynamic model of Germano (Germano *et al*., 1991). Spatial discretization is based on the scheme of the second order centered difference retaining the kinetic energy and the integration time is performed by the method of fractional step. Equations are time advanced by using a two-level explicit Adams–Bashforth scheme for the non-linear convection terms and an implicit Crank–Nicolson method for the diffusion terms. The time step used is $\Delta t = 0.005(R/U_b)$. The JetCode program calculates by mean of LES only the resolved part of turbulence intensities; the statistical quantities are calculated by averaging over time, as well as the homogeneous directions: axial and streamwise in case of plane channel, axial and azimuthal in case of a straight pipe, spanwise in case of channel with a step and azimuthal for pipe with a sudden expansion pipe. Statistical samples are collected at every time step, in all cases statistics are collected only after the flow has reached a statistically steady state and only mean quantities are calculated during the runtime; statistics quantities like root mean squares (rms) are evaluated in a post-processing routine. In this case, $u_{i\,rms}$ is the "Ith" velocity component root mean and it is calculated as $u_{i\,rms} = [(\bar{u}_i - <\bar{u}_i>)^2]^{1/2}$, where $\bar{u}_i$ is the filtered fluid velocity and $\langle u_i \rangle$ is its spatial-time average.

For particles, root mean squares of velocity are calculated in a post processing routine too, as:

$u_{i\,p\,rms} = [(\bar{u}_{i\,p} - <\bar{u}_{i\,p}>)^2]^{1/2}$ where $<\bar{u}_{i\,p}>$ is the ensamble averaged particle velocity.

2.2 Equations for the Dispersed Phase and Lagrangian Particle Tracking

In the Lagrangian framework, the motion of particles is described by a set of ordinary differential equations for particle position $\boldsymbol{x_p}$ and velocity $\boldsymbol{u_p}$. Taking into account the drag force and particle inertia (Maxey and Riley, 1983), these equations in vector form read as:

$$\frac{d\boldsymbol{x_p}}{dt} = \boldsymbol{u_p} \tag{1}$$

$$\frac{d\boldsymbol{u_p}}{dt} = \boldsymbol{g} - \frac{\left(1 + 0.15 Re_p^{0.687}\right)}{\tau_p}\left(\boldsymbol{u_p} - \boldsymbol{u}\right). \tag{2}$$

where $\boldsymbol{u}$ is the fluid velocity at the particle position, $\boldsymbol{g}$ is the gravitational acceleration vector and $\tau_p = \rho_p d_p^2/18\mu$ is the particle relaxation time (d_p and μ being the diameter of the particle and the dynamic viscosity of the fluid, respectively). The Stokes drag coefficient is computed by using a standard non-linear correction required when the particle Reynolds number, $Re_p = |\boldsymbol{u} - \boldsymbol{u_p}| d_p/\nu$ does not remain small.

In the cylindrical coordinates reference system, the left side of Eq. (2), it can be rewritten as:

$$\frac{d\boldsymbol{u_p}}{dt} = \frac{du_p}{dt}\hat{i} + \frac{dv_p}{dt}\hat{e}_r + \frac{dw_p}{dt}\hat{e}_\theta \tag{3}$$

This reference system is linked to the particle and is no inertial, also the axial coordinate (z) is uncoupled from the radial (r) and azimuthal (θ) coordinate, such that:

$$\frac{d\boldsymbol{u_p}}{dt} = \frac{du_p}{dt}\hat{i} + \frac{dv_p}{dt}\hat{e}_r + v_p\frac{d\hat{e}_r}{dt} + \frac{dw_p}{dt}\hat{e}_\theta + w_p\frac{d\hat{e}_\theta}{dt} \quad (4)$$

where, $d\hat{e}_r/dt = -\omega_p\hat{e}_r$ and $d\hat{e}_\theta/dt = \omega_p\hat{e}_\theta$, further $w_p = \omega_p r_p$, then the system of governing equations of particle movement, is expressed as:

$$\frac{dx_p}{dt}\hat{i} + \frac{dr_p}{dt}\hat{e}_r + \frac{d\theta_p}{dt}\hat{e}_\theta = u_p\hat{i} + v_p\hat{e}_r + \left(\frac{w_p}{r_p}\right)\hat{e}_\theta \quad (5)$$

$$\frac{du_p}{dt}\hat{i} + \frac{dv_p}{dt}\hat{e}_r + \frac{dw_p}{dt}\hat{e}_\theta = (g_x - F_{dx})\hat{i} + \left(g_r - F_{dr} + \frac{w_p^2}{r_p}\right)\hat{e}_r + \left(g_\theta - F_{d\theta} - \frac{w_p v_p}{r_p}\right)\hat{e}_\theta \quad (6)$$

The solution of scalar equations in r and θ has a singularity for r_p=0, to avoid this problem, it has been considered than the term $1/r_p \neq 0$ for values of $r_p > \epsilon$ with $\epsilon = r_{pmín}$ being $r_{pmín}$ the smallest particle radio used in simulations, so this has to be set previously by the Langragian module user.

To calculate individual particle trajectories, the Lagrangian tracking routine is coupled to the JetCode program, it contains the steps described by Yeung and Pope (1988) to solve the motion equations of the disperse phase. The routine solves Eqs. (6) and (5) under the following assumptions: (i) particles are pointwise, non-rotating rigid spheres; (ii) particles are injected into the flow at concentration low enough to consider dilute flow: the effect of particles onto the turbulent field is neglected (one-way coupling approach) iii) inter-particle collisions are neglected; iv) perfectly-elastic collisions at the smooth walls are assumed when the particle center is at a distance lower than one particle radius from the wall (Marchioli and Soldati, 2002).

The equations of particle motion are time advanced by a 4th-order Runge–Kutta scheme: at the beginning, particles are randomly distributed over the injection area with disk shape (see Fig. 1) and their initial velocity is set equal to the filtered fluid velocity at the particle initial position (assuming that the flow field is not locally disturbed around the particle (Gatignol, 1983; Maxey and Riley, 1983). In our study, fluid velocity interpolation is performed using a trilinear interpolation scheme at the position of each particle (Wang and Squires, 1996) (Yamamoto *et al.*, 2001). The time step for particle tracking was chosen as equal to that of the fluid, and periodic boundary conditions were imposed on particles moving in the homogeneous (azimuthal) direction. Upon initial injection, particles need to adapt to the flow and to forget their initial conditions, statistics were collected once the number of particles within the expansion became steady.

2.3 Relationship Between the Stokes Numbers and Mean drift Parameter with Particle Dispersion in the Turbulent Recirculation Zone.

In 1992, Hardalupas *et al.* (1992), found that particle dispersión is enhanced by local air turbulence near of the recirculation bubble while particle transit time across the recirculation zone and centrifugal effects due to the curvature of the air streamlines can reduce particle dispersion into the recirculation zone. All these effects can be expressed in the form of the next Stokes number based on three different timescales of fluid:

- Large eddy Stokes number (St_e), is based on the characteristic timescale of the large eddies and the particle relaxation time. The flow timescale is the relationship between the size of the step (H) to the bulk velocity in the cross section of the expansion (U_e):

$$St_e = (U_e / H)/\tau_p \quad (7)$$

- Transit Stokes number (St_{tr}), if the particle is responsive to the flow turbulence its transit time over the distance between the step and the reattachment point must be longer than particle response time. This effect can be quantified by:

$$St_{tr} = (\tau_{tr})/\tau_p \quad (8)$$

$\tau_{tr} = x_r/\frac{1}{2}(Uc_{x=0} + Uc_{x=x_r})$ and Uc the average fluid velocity at the center line of the expansion.

- Centrifugal Stokes number (St_ω) quantifies the relative magnitude of the centripetal force to the viscous drag force acting on the particle. It can be estimated by:

$$St_\omega = (\tau_\omega)/\tau_p \quad (9)$$

τ_ω is the centrifugal timescale, defined as $1/\omega$, where ω is the angular velocity which would have the fluid movement around a notional circle of radius R that hypothetically would be tangent to the inlet pipe and would pass through the reattachment point. Hardalupas *et al.* (1992) states that for particles with $St_e O(1)$, $St_{tr} > 1$ and $St_\omega > 1$, the concentration in the recirculation zone grows abruptly.

Starting this statement, Siu *et al.* (2011) studied experimentally, the mean drift parameter, (γ_{mean}) to predict the increment of the particle concentration within the recirculation zone , which is intended to characterize the ability of the reverse bulk axial velocity of fluid to reverse also the direction of the axial velocity of the particles in the direction of the step, particularly within the recirculation zone . This parameter is defined as:

$$\gamma_{mean} = (\mathbf{u}_T)/\left|U_{b\ max}^{recirculation\ zone}\right| \quad (10)$$

where $\mathbf{u}_T$ is the terminal velocity of particles which measures the effect of the weight of the particle and is defined as the final velocity achieved by a particle

in free fall under the influence of the acceleration of gravity **g**, it is determined as:

$$\mathbf{u}_T = \tau_p \mathbf{g} \tag{11}$$

In order to support the information that provides the calculation of the previous parameters and considering that the study was done with "one way coupling", the particle concentration C_{pr} is determined by the number of particles N_{pr} within the zone between the center and the wall from $x = 0$ to $x = X_r$ when the particle number becomes steady. The value of C_{pr} is dimensionless, it is defined as the ratio $N_{pr}/N_{pr(Re_{b2}H_1 d_{p2})}$ and will be presented in Section 3.

2.4 Solved Cases

The results presented in this paper are relative to different values of the average (bulk) Reynolds number $Re_{b1} = 10600$ corresponding to a bulk velocity $U_{b1} = 4.24\, m.s^{-1}$ and $Re_{b2} = 14000$ corresponding to a bulk velocity $U_{b2} = 14.2\, m.s^{-1}$. Therefore, we solved four different cases of turbulent air flow identified with the subscript "a" if particle diameter is 60 μm or "b" if particle diameter is 150 μm: case 1_a ($Re_{b1}H_1 d_{p1}$), case 1_b ($Re_{b1}H_1 d_{p2}$), case 2_a ($Re_{b1}H_2 d_{p1}$), case 2_b ($Re_{b1}H_2 d_{p2}$), case 3_a ($Re_{b2}H_1 d_{p1}$), case 3_b ($Re_{b2}H_1 d_{p2}$), case 4_a ($Re_{b2}H_2 d_{p1}$), case 4_b ($Re_{b2}H_1 d_{p2}$).

Two computational grids with N_x x N_r x N_θ hexahedral elements were considered: at Re_{b1} a grid was made of 384 x 256 x 128 points and at Re_{b2} a grid was made of 512 x 256 x 128 points.

The element sizes were selected taking as reference those used in similar geometries reported by Segura (2004) and Akselvoll and Moin (1995), considering the guidelines for meshing in LES (Piomelli, 2006) Too, that selection was influenced by cost considerations as the largest grid on which the simulations could be completed in a reasonable amount of time. For clarity, Fig. 2 shows only an example of computational grid, this grid has fewer points in the axial, radial and azimuthal directions than that used in the calculation, but the distribution of points is the same Figure 2 shows a structured mesh scheme as described above.

3. RESULTS

The reattachment length x_r, is calculated with the friction coefficient at the wall expansion C_f:

$$C_f = \frac{2\nu}{U_b^2}\left(\frac{\delta u}{\delta r}\right)_{wall} \tag{12}$$

and the resulting reattachment lengths X_r (where $C_f = 0$) are equal to: 23R ($Re_{b1}H_1$), 27.5R ($Re_{b1}H_2$), 21.5R ($Re_{b2}H_1$) and 26.5R ($Re_{b2}H_2$). Figure 3 shows the coefficient of friction downstream the sudden expansion evaluated over the expansion pipe wall are represented for all the resolved cases.

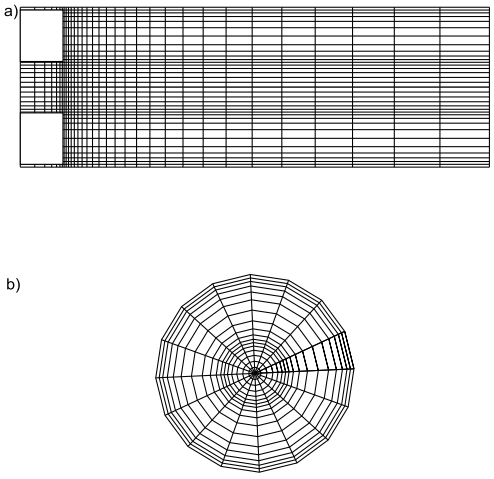

Fig. 2. Mesh scheme in (a) plane $r - z$ (b) plane $r - \theta$.

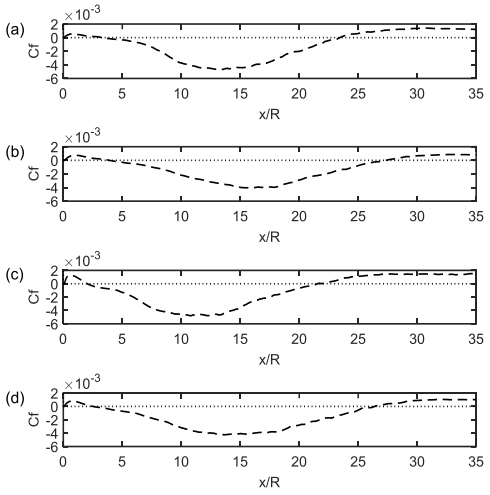

Fig. 3. Coefficient of friction evaluated over the expansion pipe wall. a) $Re_{b1}H_1$ b) $Re_{b1}H_2$ c) $Re_{b2}H_1$, d) $Re_{b2}H_2$.

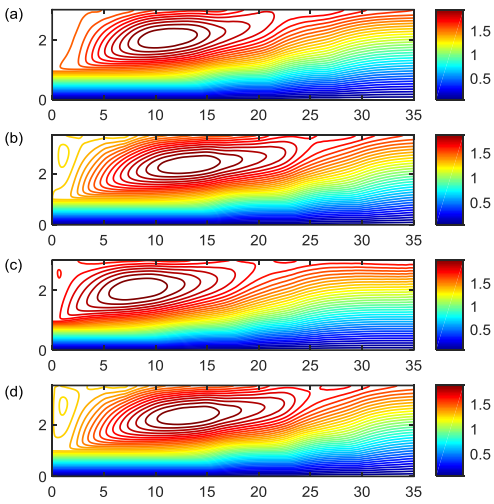

Fig. 4. Mean streamlines for a) $Re_{b1}H_1$; b) $Re_{b1}H_2$; c) $Re_{b2}H_1$; d) $Re_{b2}H_2$.

The length of the domains in both figures have been represented only up to x = 35R.

Figure 4 shows the mean streamlines along the expansion pipe for all resolved cases.

In both figures the recirculation zones are visible, focusing, key features of the flow include the primary and secondary recirculation zones are represented, exhibiting some differences between the recirculation lengths and reattachment points due Reynolds number and expansion ratio of each case. We can corroborate that if Re_b remains constant but the expansion ratio increases, the reattachment point moves downstream of the expansion and the size of the primary bubble increases. Otherwise, if the expansion ratio remains constant and increases Re_b, the size of the primary bubble decreases. The above coincides with that reported by Roy *et al.* (2010).

The velocity statistics of the fluid and particles were collected in four cross sections downstream of the expansion, located at: x = 5R, 10R, 20R and 30R, corresponding to each profiles shown from left to right in Figs. 5, 6, 7 and 8.

For brevity, only the results of cases 2_a and 2_b will be presented.

With respect to the fluid, Fig. 5 shows three different regions along the radial direction: the central region of the flow (A) where the maximum speed occurs, the transition region of the boundary layer (B) and the reverse flow zone (C) where the axial velocity is negative. As expected, farther from the sudden expansion, the radial profiles of axial fluid velocity are flat and smooth, the axial moment extends into the radial direction and velocity decays in the central zone of the flow. At x = 30R, close to the exit pipe, the flow is already in recovery zone.

The particles lead the fluid in the central zone along the entire expansion pipe which indicates that the ability of particles to adapt to the fluid motion is gradually reduced with increasing inertia. In the shear layer of the recirculation zone, particles reverse the direction of its axial velocity and follow the movement of fluid until a little beyond x=20R since $x_r = 27.5$, therefore there are particles into the recirculation zone.

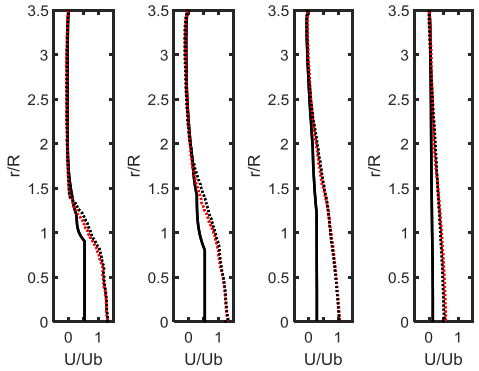

Fig. 5. Radial profiles of mean axial velocity: (-) Fluid; (··) Particles 60 μm; (··) Particles 150 μm.

Figure 6 shows radial profiles of radial velocity for both the fluid and two sizes of particles. With respect to the fluid, it is observed that the bulk radial velocity represents only a small fraction of the bulk axial velocity (shown in the previous figure), indicating that for flow solved, the motion occurs predominantly in a direction parallel to the axis of the pipe. A negative radial velocity indicates fluid movement toward the axis of the expansion, and a positive radial velocity indicates movement towards the walls. In the two first stations (x=5R and x=10R), the velocity profile is wavy, the fluid and particles suffer a radial movement toward the center of the expansion, reflecting the presence of a recirculation bubble. For particles, the positive velocity zone grows up to x=20R, which indicates that there is a particle movement to the wall expansion and into the recirculation bubble. Particles continue moving towards the wall. close to the exit expansion pipe.

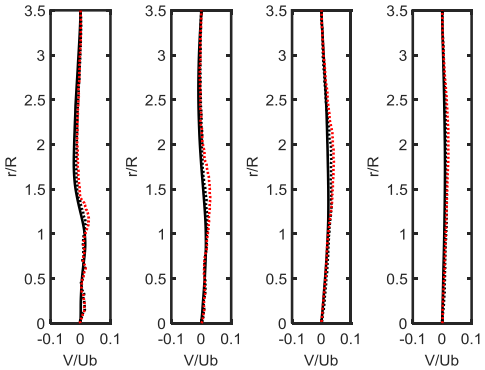

Fig. 6. Radial profiles of mean radial velocity: (-) Fluid; (··) Particles 60 μm; (··) Particles 150 μm.

Figure 7 shows the radial profile of axial velocity fluctuations; between the center and step $(R/r = 1)$, the profile of fluid axial velocity fluctuation undergoes a sharp increase close to the step, decreasing as it approaches the wall where the minimum value is located. The profiles flatten in the recovery zone, where values close to zero are to be achieved.

In the first two stations (x=5R and x=10R), the turbulent intensity in the axial direction of the particles is less than the fluid along the entire radius of the expansion and profiles exhibit a maximum peak whose location does not match the phase of transport, it also shows that in the center of the duct, particles fluctuation is much smaller than that of the fluid in those same locations. In the last two stations, close to the centerline of the pipe the particle fluctuation is less than that of the fluid and closer to the wall both fluctuations are very similar.

Figure 8, shows the radial profiles of radial fluctuating fluid velocity have its minimum value located in the expansion pipe wall and have a clearly defined peak value at the first station, from there the radial fluctuation increases along the radial direction but is attenuated as it approaches the region of recovery, which looks like a flatter profile.

The radial fluctuation of the particles is smaller than that of the fluid and changes just a little between different stations.

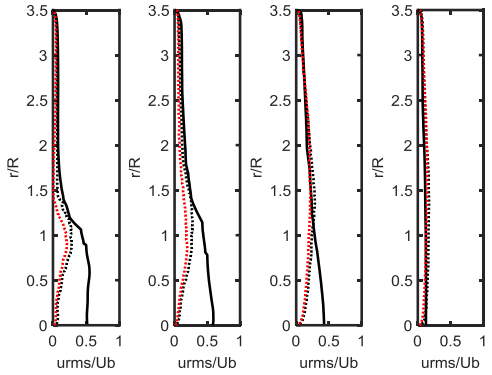

Fig. 7. Root mean square of axial velocity fluctuations: (-) Fluid; (··) Particles 60 μm; (··) Particles 150 μm.

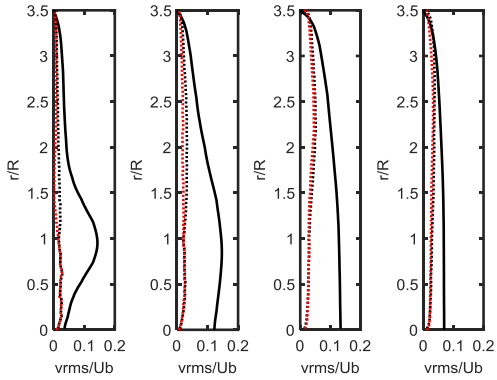

Fig. 8. Root mean square of radial velocity fluctuations: (-) Fluid; (··) Particles 60 µm; (··) Particles 150 µm.

Table 2, contains the different definition of Stokes numbers mentioned in a previous section, mean drift parameter and particle concentration within the recirculation zone for all the solved multiphase flow cases.

Table 2 Stokes numbers, mean drift parameter and solid particle concentration C_{pr} within reattachment zone

Cases	St_e	St_{tr}	St_ω	γ_m	C_{pr}
Case 1a	5.1	11.5	44.4	0.38	8.4
Case 1b	0.62	1.4	5.4	3.11	2.4
Case 2a	6.4	23.4	82.6	0.44	11.7
Case 2b	0.77	2.8	10.1	3.63	4.1
Case 3a	0.46	0.9	10.2	0.11	1.1
Case 3b	0.06	0.1	1.3	0.91	1
Case 4a	0.78	1.3	9.8	0.14	1.7
Case 4b	0.09	0.17	1.2	1.15	1.5

We can see in the above table that, comparing cases "a" (d_{p1}) with cases "b" (d_{p2}), the transit Stokes number is lower for larger particles because of the dominance of inertia; meanwhile, the effect of the curvature of the streamline that defines the recirculation zone, which indicates the relationship between the centripetal force and the inertia forces, causes that particles of higher diameter are more affected by the curvature and exhibiting lower St_ω, which probably influences their income within the recirculation zone. Also, particle concentration in the recirculation zone (C_{pr}) exhibits a maximum for Case 1a and Case 2a, which coincides with experimental findings of Hardalupas *et al.* (1992), i.e., if $St_e(O(1))$, St_{tr} *y* $St_\omega > 1$ then C_{pr} increases. Additionally, as the velocity of flow, step size and particle diameter increase and C_{pr} decreases.

The isolated effect of the drift average parameter is analyzed for cases 3 and 4, where no more than 1 simultaneous value for St_e, St_{tr} and St_ω are reached; it is observed that the decrease of this parameter matches with a higher concentration of particles within the circulation zone, which indicates that the effect of the particle weight is lower than the capacity of the reverse axial velocity of the fluid in the recirculation zone to reverse axial velocity particles, therefore more particles enter that zone. All the above coincides with findings of Siu *et al.* (2011).

Figure 9 shows the instantaneous contours of fluid axial velocity and the corresponding instantaneous particle position in the middle plane (the expansion is from $x = 0$) for smaller accumulation in the recirculation zone (Case 3b: $Re_{b2}H_1d_{p2}$). That captions correspond to a statistically steady state for the fluid phase and particles too, i.e., the number of particles entering the expansion is approximately equal to the number that leaves it.

In this case, particle Stokes numbers $St_{e,}$ St_{tr} and St_ω are not greater than 1 simultaneously, therefore they do not respond to the action of the different effects of turbulent flow. Particles are injected with the same velocities as the gas phase at the inlet of the straight pipe, however, majority of them follow the main axial flow without entering to the recirculation zone with X_r =21.5R.

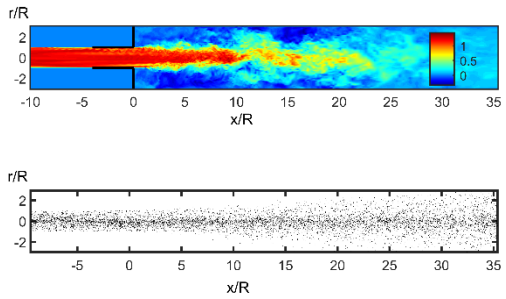

Fig. 9. Instantaneous contours of axial velocity and particle position for $Re_{b2}H_1dp_2$.

Figure 10 shows the instantaneous contours of fluid axial velocity and the corresponding instantaneous particle position in the middle plane for greater accumulation in the recirculation zone (Case 2a : $Re_{b1}H_2d_{p1}$)). That captions correspond to a statistically steady state for the fluid phase and solid particles.

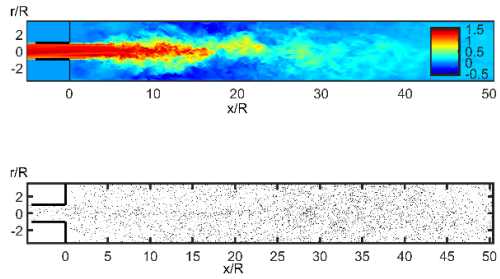

Fig. 10. Instantaneous contours of axial velocity and particle position for $Re_{b1}H_2dp_1$.

We can see that particles represented above with $St_{e,}(O(1))$, $St_{tr}\ y\ St_{\omega} > 1$ respond to the action of large eddies, flow turbulence and to the centripetal force exerted by the recirculation bubble and therefore accumulate inside the recirculation zone with $X_r = 27.5R$. That particles are carried and follow the gas phase and respond to the reversal flow as soon as they enter to the recirculation zone, spreading in the radial and azimuthal directions.

4. CONCLUSION

In this paper, we address the problem of quantifying the solid particle dispersion in the turbulent recirculation zone of a sudden expansion pipe by means of Stokes numbers and mean drift parameter. For this purpose, statistics of fluid and particle velocity were obtained from large eddy simulation of turbulent flow in a vertical and downward sudden expansion pipe and particle Lagrangian tracking. Different flow configurations (Reynolds numbers, step sizes and particle diameter) were studied. The results within the assumptions made, allow to conclude as follows: statistics fluid and particle velocity were adequately solved, showing that the fluid is more sensitive to the negative gradient pressure and particles to gravity. In the central area of the flow, both sizes of particles do not seem to be very sensitive to turbulent fluctuations of the fluid, which attenuate more rapidly along the expansion than the particles (without reference to modulating the turbulence of the transport phase due to the presence of the dispersed phase).

We calculated Stokes numbers based on different fluid timescales and mean drift parameter and checked that the simultaneous values greater than 1 of the large eddy, centrifugal and transit Stokes numbers, determine an increasing of particle concentration within the turbulent recirculation zone. Also, the isolated effect of the mean drift parameter was studied concluding that its decrease determines an increasing of particle concentration within the turbulent recirculation zone regardless the different Stokes numbers are greater than 1. Finally, the solid particle dispersion within the turbulent recirculation zone in a sudden expansion pipe using dimensionless parameters was numerically characterized.

REFERENCES

Aguinaga, S., J. Borée, O. Simonin, J. P. Bouchet and V. Herbert (2008). Droplets dispersion and deposition measurements in an axisymmetric sudden expansion flow. *Proceedings 14th Int. Symp. on Applications of Laser Techniques to Fluid Mechanics*. Portugal, 1-12.

Ahmadi, G. and Q. Chen (1998). Dispersion and deposition of particles in a turbulent pipe flow with sudden expansion. *Journal of Aerosol Science* 29(9), 1097-1116.

Akselvoll, K. and P. Moin (1995). *Large eddy simulation of turbulent confined coannular jets and turbulent flow over a backward facing step*. Report No. TF-63, Mechanical Engineering Department, Stanford University. USA.

El-Askary, W. A., I. M. Eldesoky, O. Saleh, S. M. El-Behery and A. S. Dawood (2015). Behavior of downward turbulent gas-solid flow through sudden expansion pipe. *Powder Technology* 291, 351-365.

Fessler, J. R. and J. K. Eaton (1997). Particle response in a planar sudden expansion flow. *Experimental Thermal and Fluid Science* 15(4), 413-423.

Founti, M. and A. Klipfel (1998). Experimental and computational investigations of nearly dense two-phase sudden expansion flows. *Experimental Thermal and Fluid Science* 17(1-2), 27-36.

Gatignol, R. (1983). The Faxén formulae for a rigid particle in an unsteady non-uniform Stokes flow. *Journal de Mécanique Théorique et Appliquée.* 1(2), 143-160.

Germano, M., U. Piomelli, P. Moin and W. H. Cabot (1991). A dynamic subgrid-scale eddy viscosity model. *Physics of Fluids* 3(7), 1760-1765.

Hardalupas, Y., A. M. K. P. Taylor and J. H. Whitelaw (1992). Particle dispersion in a vertical round sudden-expansion flow. *Philosophical Transactions of the Royal Society of London* 341(1662), 411-442.

Kulick, J., J. R. Fessler and J. K. Eaton (1994). Particle response and turbulence modification in fully developed channel flow. *Journal of Fluid Mechanics* 277, 109-134.

Lau, T. C. W. and G. J. Nathan (2014). Influence of Stokes number on the velocity and concentration distribution in particle laden jets. *Journal of Fluid Mechanics* 757, 432-457.

Marchioli, C. and A. Soldati (2002). Mechanisms for particle transfer and segregation in a turbulent boundary layer. *Journal of Fluid Mechanics* 468, 283-315.

Marchioli, C., A. Giusti, M. V. Salvetti and A. Soldati (2003). Direct numerical simulation of particle wall transfer and deposition in upward turbulent pipe flow. *International Journal of Multiphase Flow* 29(6), 1017-1038.

Maxey, M. R. and J. J. Riley (1983). Equation of motion for a small rigid sphere in nonuniform

flow. *Physics of Fluids* 174, 441-465.

Mergheni, M. A., J. Ch. Sautet, T. H. Ben and N. S. Ben (2012). Numerical simulation of sudden-expansion particle-laden flows using the Eulerian-Lagrangian approach. *Thermal Science* 26(4), 1005-1012.

Pakhomov, M. A. and V. I. Terekhov (2013). Second moment closure modelling of flow, turbulence and heat transfer in droplet laden mist flow in a vertical pipe with sudden expansion. *International Journal of Heat and Mass Transfer* 66, 210-222.

Pierce, C. D. and P. Moin (2001). *Progress-variable approach for large eddy simulation of turbulent combustion*. Report No. TF-80, Mechanical Engineering Department, Stanford University.

Piomelli, U. (2006). *Large Eddy Simulations and related techniques theory and applications*. Lecture series 2006-04. Von Kàrman Institute for Fluid Dynamics.

Roy, V., S. Majumder and D. Sanyal (2010). Analysis of the turbulent fluid flow in an axi-symmetric sudden expansion. *International Journal of Engineering Science and Technology* 2(6), 1569-1574.

Segura, J. (2004). *Predictive capabilities of particle laden large eddy simulation*. Ph. D. thesis, Stanford University. USA

Siu, Y. W. and A. M. K. P. Taylor (2011). Particle capture by turbulent recirculation zones measured using long-time Lagrangian particle tracking. *Experiments in Fluids* 51(1), 95-121.

Tashiro, H. and Y. Tomita (1986). Influence of diameter ratio on a sudden expansion of a circular pipe in gas-solid two-phase flow. *Powder Technology* 48(3), 227-231.

Terekhov, V. I. and M. A. Pakhomov (2008). Turbulent gas-dispersed flow in a pipe with sudden expansion: numerical simulation. *Thermophysics and Aeromechanics* 15(4), 589-601.

Torres, M. J. (2014). *Numerical study of turbulent flow laden with solid particles in channel and pipes with variable section*. PhD Thesis. Universidad Politécnica de Madrid

Wang, L. P. and D. E. Stock (1993). Dispersion of heavy particle by turbulent motion. *Journal of Atmospheric Sciences* 50(13), 1897-1913.

Wang, Q. and K. D. Squires (1996). LES of particle-laden channel flow. *Physics of Fluids* 8(5), 1207-1223.

Yamamoto, Y., Potthoff, M., Tanaka, T., Kajishima (2001). Large-eddy simulation of gas-particle flow in a vertical channel: effect of considering inter-particle collisions. *Journal of Fluid Mechanics* 442, 303-334.

Yeung, P. K. and S. B. Pope (1988). An algorithm for tracking fluid particles in numerical simulations of homogeneous turbulence. *Journal of Computational Physics* 79(2), 373-416.